Applications of Mathematics

Ladislav Foltyn; Dalibor Lukáš; Ivo Peterek
Domain decomposition methods coupled with parareal for the transient heat equation in 1 and 2 spatial dimensions

DOMAIN DECOMPOSITION METHODS COUPLED WITH PARAREAL FOR THE TRANSIENT HEAT EQUATION IN 1 AND 2 SPATIAL DIMENSIONS

Ladislav Foltyn, Dalibor Lukáš, Ivo Peterek, Ostrava

Abstract. We present a parallel solution algorithm for the transient heat equation in one and two spatial dimensions. The problem is discretized in space by the lowest-order conforming finite element method. Further, a one-step time integration scheme is used for the numerical solution of the arising system of ordinary differential equations. For the latter, the parareal method decomposing the time interval into subintervals is employed. It leads to parallel solution of smaller time-dependent problems. At each time slice a pseudo-stationary elliptic heat equation is solved by means of a domain decomposition method (DDM). In the $2d$, case we employ a nonoverlapping Schur complement method, while in the $1d$ case an overlapping Schwarz DDM is employed. We document computational efficiency, as well as theoretical convergence rates of FEM semi-discretization schemes on numerical examples.

Keywords: domain decomposition method; parareal method; finite element method; heat equation

MSC 2020: 65N55, 65N30, 65F08

1. Introduction

Domain decomposition methods (DDM) are well-established techniques of parallel numerical solution to linear boundary value problems for elliptic partial differential equations (PDE). The problem is typically discretized by means of the finite element method leading to a system of linear equations. The discretization usually aligns with a decomposition of the computational domain into either overlapping [21] or nonoverlaping [23] subdomains. This results in a number of PDE subproblems that can be solved in parallel. The concurrent subproblems are coupled via a global coarse

problem of a much smaller size than the original system. In case of nonoverlapping DDM, there are methods of balancing domain decomposition [17], finite element tearing and interconnecting [5], or Schur complement methods [1], to name a few. All these methods combine direct methods for the subdomain and coarse problems to build a preconditioner for an iterative method applied to the original large system. The condition number of such a preconditioned system is only poly-logarithmic in terms of H/h, where H is a typical subdomain diameter and h denotes the FEM discretization step. The methods enjoy strong parallel scalability, meaning that both the computational time and memory consumption is inversely proportional to the number of computational cores.

The situation becomes more difficult in case of time-evolving PDEs. Due to the fact that the solution to an evolution problem at a time instance depends only on the previous time instances it was believed that it would not be possible to break this sequential nature and develop a parallel solution algorithm. In 2001, Lions, Maday, and Turinici published a breakthrough paper [13] in this regard. They introduced the parareal method for parallel-in-time solution of first-order differential equations. The method decomposes the time interval into subintervals and combines concurrent local fine integrators with a global coarse integrator in the sense of a predictor-corrector technique. The convergence of the method was proven in [11]. In [12] it was proven to be super-linear on bounded and linear on unbounded time intervals. In [12] connections to the multiple shooting method, as well as the multigrid method were shown. In [4] the parareal method is presented as a two-grid Newton method. The authors further deliver a parallel speedup analysis and a feasibility study towards fluid simulations and structural analysis, the latter of which proves some instability issues. Stability for hyperbolic systems was later recovered in [2]. Many engineering applications of the parareal method were done, cf. [18], [20]. We also refer to the nice overview paper [6].

Besides the parareal method discretizing the PDE in the time direction, waveform relaxation methods have been developed. They generalize the DDM such that concurrent time-dependent local problems are solved on spatial subdomains throughout the whole time interval. Nonoverlapping Neumann-Neumann and Dirichlet-Neumann Schwarz methods applied to 1-dimensional heat equation with some preliminary results in 2 dimensions are presented in [9]. The overlapping Schwarz applied to 1-dimensional wave equation is presented in [7], [8].

Finally, much interesting work has been done in the direction of parallel-in-time multigrid methods. In [19], [10] a parallel space-time multigrid method is proposed and analyzed for the discontinuous-in-time and continuous-in-space Galerkin method for parabolic problems. Numerical results proving parallel scalability up to billions of degrees of freedom are given for the 2-dimensional heat equation as well as

Navier-Stokes equations with geometry evolving in time. Another approach combining a finite-difference multigrid method in space with the parareal method is presented in [3].

In this paper, we propose a combination of the parareal method and DDM for the heat equation. In Section 2, we recall the weak formulation of the heat equation, we discretize it by the finite element method in space, and we recall the convergence theory of the FEM approximations towards the space-time weak solution. In Section 3, we recall the parareal method, a 2-dimensional nonoverlapping Schur complement method and a 1-dimensional overlapping Schwarz DDM. In Section 4, we present numerical results confirming the FEM convergence theory, the efficiency of the parareal method, and its combination with two DDMs. This combination is the novelty of the paper. We show that the efficiency of the parareal method, i.e., super-linear convergence with respect to the number of time subintervals, is preserved as long as the precision of the nested domain decomposition solved is high enough. Our results are similar for both the 2-dimensional nonoverlapping Schur complement DDM and the 1-dimensional overlapping Schwarz DDM. Regarding related attempts in literature, to our best knowledge, the combination of parareal and the Schur complement DDM has never been studied. A variant of the combination of the parareal and an overlapping Schwarz has been presented in [15], [16]. Their setup is simpler; only two spatial subdomains, with an extra domain treated as overlap, are considered and a single Schwarz iteration is performed within a step of the parareal method.

2. FINITE ELEMENT SEMI-DISCRETIZATION OF THE TRANSIENT HEAT EQUATION

We consider the following initial boundary value problem for the heat equation:

$$(2.1) \quad \begin{cases} c(x)\dfrac{\partial u}{\partial t}(x,t) - \text{div}(\nu(x)\nabla u(x,t)) = f(x,t), & x \in \Omega, \ t \in I, \\[2mm] u(x,t) = 0, & x \in \Gamma_\text{D}, \ t \in I, \\[2mm] \nu(x)\dfrac{\partial u}{\partial n}(x,t) = g(x,t), & x \in \Gamma_\text{N}, \ t \in I, \\[2mm] u(x,0) = u_0(x), & x \in \Omega, \end{cases}$$

where we search for the temperature distribution $u(x,t)$ in the spatial domain $\Omega \subset \mathbb{R}^d$, $d = 1, 2$, and the time interval $I := (0,T)$. The functions $c(x)$ and $\nu(x)$ are the spatial distributions of the heat capacity and the heat conductivity, respectively, and $f(x,t)$ denotes the volume heat sources. The boundary $\Gamma := \partial\Omega$ is decomposed into two nonoverlapping components—the Dirichlet part Γ_D, on which we prescribe the zero temperature, and the Neumann part Γ_N, on which a numerical flux g is

prescribed. By n we denote the unit normal vector outward to Ω, and u_0 is the spatial distribution of the initial temperature.

Let $V := H^1_{0,\Gamma_D}(\Omega) = \{v \in L^2(\Omega)\colon \nabla v \in [L^2(\Omega)]^d, \; v = 0 \text{ on } \Gamma_D\}$, where the gradient is in the distributional sense and the boundary values are in the sense of traces. We denote the dual space of V by V^*. The weak formulation of (2.1) reads to find $u \in L^2(I, V)$ such that $\partial u/\partial t \in L^2(I, V^*)$, $u(x,0) = u_0(x)$ a.e. in Ω, and for almost all $t \in I$:

$$
(2.2) \qquad \int_\Omega c(x) \frac{\partial u}{\partial t}(x,t) v(x) \, \mathrm{d}x + \int_\Omega \nu(x) \nabla u(x,t) \cdot \nabla v(x) \, \mathrm{d}x
$$
$$
= \int_\Omega f(x,t) v(x) \, \mathrm{d}x + \int_{\Gamma_N} g(x,t) v(x) \, \mathrm{d}s(x) \quad \forall\, v(x) \in V.
$$

The following theorem is a direct consequence of [24], Theorem 23.A.

Theorem 2.1. *Let $I := (0, T)$, $T > 0$, and let $\Omega \subset \mathbb{R}^d$, $d = 1, 2$, be a bounded simply-connected domain with Lipschitz boundary, which consists of two nonoverlapping Lebesgue measurable components Γ_D and Γ_N with $\mathrm{meas}\,\Gamma_D > 0$. Assume further that $u_0 \in L^2(\Omega)$, $f \in L^2(\Omega \times I)$, $g \in L^2(\Gamma_N \times I)$, and $c, \nu \in L^\infty(\Omega)$ be such that $c(x) \geqslant c_0 > 0$ and $\nu(x) \geqslant \nu_0 > 0$ a.e. in Ω. Then there exists a unique solution u to (2.2), which continuously depends on the data, i.e., there exists $C > 0$ such that*

$$
\|u\|_{L^2(I;V)} + \|u'\|_{L^2(I;V^*)} \leqslant C(\|u_0\|_{L^2(\Omega)} + \|f\|_{L^2(\Omega \times I)} + \|g\|_{L^2(\Gamma_N \times I)}).
$$

We recall that the norm in the Bochner-Lebesgue space $L^2(I, B)$, where B is a Banach space, is defined as follows:

$$
\|u\|_{L^2(I;B)} := \left(\int_I \|u(t)\|_B^2 \, \mathrm{d}t \right)^{1/2}.
$$

We introduce a shape-regular and quasi-uniform finite element triangulation of Ω and the conforming finite element subspace $V^h := \mathrm{span}(\varphi_1(x), \ldots, \varphi_n(x)) \subset V$, where $\varphi_i(x)$ is the element-wise linear nodal FEM basis function. The Galerkin approximation of (2.2) results in the following Cauchy problem for linear system of the first-order ordinary differential equations:

$$
(2.3) \qquad \begin{cases} \mathbf{M}\mathbf{u}'(t) + \mathbf{K}\mathbf{u}(t) = \mathbf{b}(t) & \forall\, t \in I, \\ \mathbf{u}(0) = \mathbf{u}_0, \end{cases}
$$

where the entries of $\mathbf{M}$, $\mathbf{K}$, and $\mathbf{b}$, respectively, read as follows: $(\mathbf{M})_{ij} := \int_\Omega c \varphi_j \varphi_i$, $(\mathbf{K})_{ij} := \int_\Omega \nu \nabla \varphi_j \nabla \varphi_i$, and $(\mathbf{b}(t))_i := \int_\Omega f(t) \varphi_i + \int_{\Gamma_N} g(t) \varphi_i$ for $i, j = 1, \ldots, n$. The

function $u_0^h(x) := \sum_{j=1}^{n} (\mathbf{u}_0)_j \varphi_j(x)$ is an approximation of $u_0(x)$. The approximate solution reads as follows:

$$(2.4) \qquad u^h(x,t) := \sum_{j=1}^{n} (\mathbf{u}(t))_j \varphi_j(x).$$

Note that the unique solvability of problem (2.3) follows from the fact that both $\mathbf{M}$ and $\mathbf{K}$ are symmetric positive definite.

From [22], Theorems 1.2 and 1.3 we have the following convergence result.

Theorem 2.2. *Let the assumptions of Theorem 2.1 hold true. Further, let* $\Gamma_D := \Gamma$, *i.e.,* $\Gamma_N = \emptyset$, u^h *be the solution to (2.3), (2.4), and u be the solution to (2.2). Assume $u_0^h = 0$ on Γ. Then there exists $C > 0$ independent of h such that for $r \in \{1,2\}$ and $t \geqslant 0$:*

$$\|u^h(x,t) - u(x,t)\|_{L^2(\Omega)} \leqslant \|u_0^h(x) - u_0(x)\|_{L^2(\Omega)}$$
$$+ Ch^r \left(\|u_0(x)\|_{H^r(\Omega)} + \int_0^t \left\| \frac{\partial u}{\partial s}(x,s) \right\|_{H^r(\Omega)} \mathrm{d}s \right)$$

and

$$\|\nabla u^h(x,t) - \nabla u(x,t)\|_{L^2(\Omega)} \leqslant \|\nabla u_0^h(x) - \nabla u_0(x)\|_{L^2(\Omega)}$$
$$+ Ch^{r-1} \left\{ \|u_0(x)\|_{H^r(\Omega)} + \|u(x,t)\|_{H^r(\Omega)} + \left(\int_0^t \left\| \frac{\partial u}{\partial s}(x,s) \right\|_{H^{r-1}(\Omega)}^2 \mathrm{d}s \right)^{1/2} \right\}.$$

Finally, we employ time-stepping schemes. We decompose I into m time intervals (t_{k-1}, t_k), where $t_k := k\delta t$, $k = 0, 1, \ldots, m$, and $\delta t := T/m$. In the backward Euler time-stepping method, the time derivative is approximated by the backward difference

$$\mathbf{u}'(t_k) \approx \frac{1}{\delta t}(\mathbf{u}_k - \mathbf{u}_{k-1}),$$

where $\mathbf{u}_k := \mathbf{u}(t_k)$. Hence, we sequentially solve the following linear systems:

$$(2.5) \qquad (\mathbf{M} + \delta t \mathbf{K})\mathbf{u}_k = \delta t \mathbf{b}_k + \mathbf{M}\mathbf{u}_{k-1}, \quad k \geqslant 1,$$

where $\mathbf{b}_k := \mathbf{b}(t_k)$. The approximate solution reads

$$(2.6) \qquad u_k^h(x) := \sum_{j=1}^{n} (\mathbf{u}_k)_j \varphi_j(x).$$

From [22], Theorem 1.5 we have the following convergence result.

Theorem 2.3. *Let the assumptions of Theorem 2.2 hold true. Further, let u_k^h, $k \geqslant 0$, be the solution to (2.5), (2.6), and let there exist $K > 0$ independent of h such that for all $r \in \{1, 2\}$:*

$$\|u_0^h(x) - u_0(x)\|_{L^2(\Omega)} \leqslant Kh^r \|u_0(x)\|_{H^r(\Omega)}$$

and $u_0(x) = 0$ on Γ. Then there exists $C > 0$ such that for $k \geqslant 0$ and $r \in \{1, 2\}$ we have

$$\|u_k^h(x) - u(x, t_k)\|_{L^2(\Omega)} \leqslant Ch^r \left(\|u_0(x)\|_{H^r(\Omega)} + \int_0^{t_k} \left\| \frac{\partial u}{\partial s}(x, s) \right\|_{H^r(\Omega)} \mathrm{d}s \right)$$
$$+ \delta t \int_0^{t_k} \left\| \frac{\partial^2 u}{\partial s^2}(x, s) \right\|_{L^2(\Omega)} \mathrm{d}s.$$

A higher convergence-in-time rate can be achieved by employing the Crank-Nicolson scheme. We arrive at the following sequence of linear systems:

$$(2.7) \qquad \left(\mathbf{M} + \frac{1}{2} \delta t \mathbf{K} \right) \mathbf{u}_k = \delta t \mathbf{b}_{k-1/2} + \left(\mathbf{M} - \frac{1}{2} \delta t \mathbf{K} \right) \mathbf{u}_{k-1}, \quad k \geqslant 1.$$

From [22], Theorem 1.6 we have the following convergence result.

Theorem 2.4. *Let the assumptions of Theorem 2.2 hold true. Further, let u_k^h, $k \geqslant 0$, be the solution to (2.7), (2.6), and let there exist $K > 0$ independent of h such that for all $r \in \{1, 2\}$:*

$$\|u_0^h(x) - u_0(x)\|_{L^2(\Omega)} \leqslant Kh^r \|u_0(x)\|_{H^r(\Omega)}$$

and $u_0(x) = 0$ on Γ. Then there exists $C > 0$ such that for $k \geqslant 0$ and $r \in \{1, 2\}$ we have

$$\|u_k^h(x) - u(x, t_k)\|_{L^2(\Omega)} \leqslant Ch^r \left(\|u_0(x)\|_{H^r(\Omega)} + \int_0^{t_k} \left\| \frac{\partial u}{\partial s}(x, s) \right\|_{H^r(\Omega)} \mathrm{d}s \right)$$
$$+ C(\delta t)^2 \int_0^{t_k} \left(\left\| \frac{\partial^3 u}{\partial s^3}(x, s) \right\|_{L^2(\Omega)} + \left\| \triangle_x \left(\frac{\partial^2 u}{\partial s^2}(x, s) \right) \right\|_{L^2(\Omega)} \right) \mathrm{d}s.$$

3. Domain decomposition coupled with parareal

We introduce parallelism into the numerical solution procedures for the FEM semi-discretized system (2.3). We include parallelization in time by means of the parareal method as well as parallelization in space by means of domain decomposition methods for the auxiliary pseudo-stationary linear systems (2.5) or (2.7) arising at each time step.

3.1. Parareal. We adopt the following parallel strategy for solution to (2.3). We split the time interval $I = (0, T)$ into M nonoverlapping, for simplicity, equidistant subintervals (T_k, T_{k+1}), $k = 0, 1, \ldots, M - 1$, where $T_k := k\Delta T$ and $\Delta T := T/M$, $M \ll m$. Assume that ΔT is an integer multiple of δt. Given a solution estimate on the coarse time-grid $\mathbf{U}_k \approx \mathbf{u}(T_k)$ for $k = 0, 1, \ldots, M - 1$, where $\mathbf{U}_0 := \mathbf{u}_0$, we solve the following M problems on shorter time intervals in parallel:

$$(3.1) \qquad \begin{cases} \mathbf{M}\mathbf{v}_k'(t) + \mathbf{K}\mathbf{v}_k(t) = \mathbf{b}(t) & \forall\, t \in I_k := (T_k, T_{k+1}), \\ \mathbf{v}_k(T_k) = \mathbf{U}_k. \end{cases}$$

In this way we predict the solution $\mathbf{u}(t) \approx \mathbf{v}_k(t)$ on I_k up to the error $\mathbf{e}_k(t) := \mathbf{u}(t) - \mathbf{v}_k(t)$, which is the solution to the following homogeneous system over I:

$$(3.2) \qquad \begin{cases} \mathbf{M}\mathbf{e}_k(t) = \mathbf{0} & \forall\, t \in I_k \;\forall\, k \in \{0, 1, \ldots, M - 1\}, \\ \mathbf{e}_k(T_k) - \mathbf{e}_{k-1}(T_k) = \mathbf{v}_{k-1}(T_k) - \mathbf{U}_k & \forall\, k \in \{1, 2, \ldots, M - 1\}, \\ \mathbf{e}_0(0) = \mathbf{0}. \end{cases}$$

Notice that the solution to problem (3.2) would lead to a sequential procedure, the computational cost of which is the same as that of solution to the original problem (2.3). Therefore, in the parareal method we solve (3.2) only approximately. The idea of the parareal method [13] is to alternate the predictor, which is the numerical solution to (3.1) using the fine scheme with time-step δt, and the corrector, which is the approximate solution to (3.2) using a coarse scheme, typically with time-step ΔT. Obviously, after i such predictor-corrector steps we get the discretized solution on $[0, T_i]$. Nevertheless, the parareal method converges super-linearly [11] with respect to ΔT also on the yet unresolved interval $(T_i, T]$. In fact, the parallel speedup, i.e. the number of parallel processes times the ratio between the computational time of the sequential algorithm and the computational time of the parallel one, is roughly inversely proportional to the number of iterations, cf. [4].

We shall summarize the parareal algorithm. Denoting by $\boldsymbol{\mathcal{I}}_{\delta t}(T_k, T_{k+1}, \mathbf{b}, \mathbf{U}_k)$ a one-step numerical solution procedure to (3.1) and assuming the same one-step

method for the solution of (3.2), but now with the time-step ΔT,

$$\mathcal{I}_{\Delta T}(T_k, T_{k+1}, \mathbf{0}, \underbrace{\mathbf{e}_{k-1}(T_k) + \mathbf{v}_{k-1}(T_k) - \mathbf{U}_k}_{=\mathbf{e}_k(T_k)})$$

the parareal method can be written in the following condensed form: Given the initial coarse prediction $\mathbf{U}_{k+1}^0 := \mathcal{I}_{\Delta T}(T_k, T_{k+1}, \mathbf{b}, \mathbf{U}_k^0)$ with $\mathbf{U}_0^0 := \mathbf{u}_0$, the ith iteration of the parareal reads

$$(3.3) \qquad \mathbf{U}_{k+1}^{i+1} = \underbrace{\mathcal{I}_{\delta t}(T_k, T_{k+1}, \mathbf{b}, \mathbf{U}_k^i)}_{=:\mathbf{U}_{k+1}^{i+1/2} \approx \mathbf{v}_k(T_{k+1})} + \mathcal{I}_{\Delta T}(T_k, T_{k+1}, \mathbf{0}, \underbrace{\mathbf{U}_k^{i+1} - \mathbf{U}_k^i}_{\approx \mathbf{e}_k(T_k)})$$

for $k = 0, 1, \ldots, M - 1$. The first term on the right-hand side of (3.3) is the fine-grid predictor while the rest is the coarse-grid corrector, which, e.g., in case of the backward Euler method (2.5) reads as follows:

$$\left(\frac{1}{\Delta T}\mathbf{M} + \mathbf{K}\right) \underbrace{(\mathbf{U}_{k+1}^{i+1} - \mathbf{U}_{k+1}^{i+1/2})}_{\approx \mathbf{e}_k(T_{k+1})}$$

$$-\frac{1}{\Delta T}\mathbf{M}\underbrace{\left[\underbrace{(\mathbf{U}_k^{i+1} - \mathbf{U}_k^{i+1/2})}_{\approx \mathbf{e}_{k-1}(T_k)} + \underbrace{(\mathbf{U}_k^{i+1/2} - \mathbf{U}_k^i)}_{\approx \mathbf{v}_{k-1}(T_k) - \mathbf{U}_k}\right]}_{\approx \mathbf{e}_k(T_k)} = \mathbf{0}, \quad k = 0, 1, \ldots, M - 1,$$

where $\mathbf{U}_0^i = \mathbf{u}_0$. Hence, (3.3) indeed coincides with (3.1) and (3.2).

The overall algorithm reads:

Algorithm

$\mathbf{U}_0^0 := \mathbf{u}_0$
for $k := 0, 1, \ldots, M - 1$ **do**
$\quad \mathbf{U}_{k+1}^0 := \mathcal{I}_{\Delta T}(T_k, T_{k+1}, \mathbf{b}, \mathbf{U}_k^0)$
end for
$i := 0$
repeat
$\quad \mathbf{U}_{k+1}^{i+1/2} := \mathcal{I}_{\delta t}(T_k, T_{k+1}, \mathbf{b}, \mathbf{U}_k^i), \ k = 0, 1, \ldots, M - 1 \quad$ % solve in parallel
$\quad \mathbf{U}_0^{i+1} := \mathbf{u}_0$
$\quad$**for** $k := 0, 1, \ldots, M - 1$ **do**
$\quad\quad \mathbf{U}_{k+1}^{i+1} := \mathbf{U}_{k+1}^{i+1/2} + \mathcal{I}_{\Delta T}(T_k, T_{k+1}, \mathbf{0}, \mathbf{U}_k^{i+1} - \mathbf{U}_k^i)$
$\quad$**end for**
$\quad i := i + 1$
until $\max_k \|\mathbf{U}_k^i - \mathbf{U}_k^{i-1/2}\| \leqslant$ tolerance

---

3.2. Domain decomposition methods. Assuming a one-step time integrator, at each time step of the temporal fine-grid predictor (3.1) as well as the coarse-grid corrector (3.2), a linear system, e.g. (2.5) or (2.7), is solved. Since it is an FEM discretization of an elliptic problem, we can employ a spatial DDM to increase the parallelism. We opt for a Schur complement method [1], [14] in the 2-dimensional case. Since in the 1-dimensional counterpart the Schur complement method is simply the direct solver, we employ an overlapping Schwarz method to verify the robustness of the parareal.

3.2.1. 2-dimensional Schur complement DDM. Let us denote the symmetric and positive-definite system arising at an iteration of the one-step time integration scheme of (2.3) by

$$(3.4) \qquad\qquad \mathbf{A}\mathbf{u} = \mathbf{b}.$$

We shall describe the domain decomposition method referring to Figure 1. We follow the presentation in [14]. We assume that besides the FEM triangulation, the computational domain $\Omega \subset \mathbb{R}^2$ is decomposed into N nonoverlapping triangular or rectangular subdomains Ω_i, $i = 1, \ldots, N$, of a typical diameter H so that the interface, the so-called skeleton, aligns with the finite element triangulation of a typical
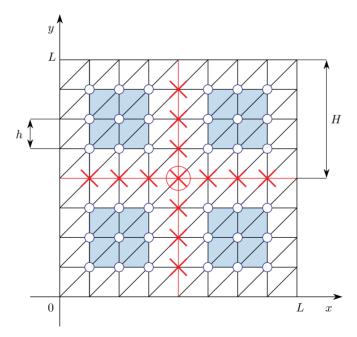

Figure 1. Discretization of the spatial domain.

diameter h, $h \ll H$. We group the FEM basis functions $\varphi_1, \ldots, \varphi_n \in V_h$ into $N + 1$ sets as follows:

▷ In the first set I_1 we take indices whose basis functions have supports in $\overline{\Omega}_1$,

▷ in the second set I_2 we collect indices whose basis functions have supports in $\overline{\Omega}_2$,

▷ ...

▷ In the set I_N we pick indices whose basis functions have supports in $\overline{\Omega}_N$.

▷ Finally, we take the remainding indices I_S whose basis functions are associated to the nodes along the skeleton or the Neumann part Γ_N of the boundary.

After this perturbation of indices, the upper-left block of the system (3.4) becomes block-diagonal, which we exploit in the following solution procedure, the first and last step of which can be performed by N concurrent processes:

(1) $\mathbf{A}_{I_i, I_i} \mathbf{u}^{\mathrm{P}}_{I_i} = \mathbf{b}_{I_i}$ for $i = 1, 2, \ldots, N$,

(2) $\mathbf{S} \mathbf{u}^{\mathrm{H}}_{I_S} = \mathbf{b}_{I_S} - \sum_{i=1}^{N} \mathbf{A}_{I_S, I_i} \mathbf{u}^{\mathrm{P}}_{I_i}$,

(3) $\mathbf{A}_{I_i, I_i} \mathbf{u}^{\mathrm{H}}_{I_i} = -\mathbf{A}_{I_i, I_S} \mathbf{u}^{\mathrm{H}}_{I_S}$ for $i = 1, 2, \ldots, N$,

where $\mathbf{S} := \mathbf{A}_{I_S, I_S} - \sum_{i=1}^{N} \mathbf{A}_{I_S, I_i} (\mathbf{A}_{I_i, I_i})^{-1} \mathbf{A}_{I_i, I_S}$. The solution (up to the permutation) is $\mathbf{u} = \mathbf{u}^{\mathrm{H}} + \mathbf{u}^{\mathrm{P}}$.

The idea of the DDM of our choice, the so-called vertex-based method [1], [23], [14], is to replace the costly Schur complement $\mathbf{S}$ by an approximation $\widehat{\mathbf{S}}$. We rely on the observation that $\mathbf{S}$ is a blockwise sparse matrix with the sparsity pattern corresponding to the graph of the skeleton. Namely, only the pairs of basis functions that are associated to a common subdomain Ω_i have a nonzero contribution in $\mathbf{S}$. To exploit this property, we number all the edges, including those along Γ_N, of the skeleton $1, 2, \ldots, N_E$ and group the skeleton indices I_S into the following subsets:

▷ In the first set I^E_1 we take indices adjacent to the interior nodes of the first edge,

▷ ...

▷ In the set $I^E_{N_E}$ we pick indices adjacent to the interior nodes of the last edge.

▷ In the set I^V we collect the remaining nodes, which are called vertices. Either they are shared by at least three subdomains, or they are end-points of a Neumann edge.

We abbreviate the union of all the edge sets by I^E. We denote the number of elements in a set I by $|I|$. Furthermore, referring to Figure 2, we replace the vertex basis functions, the support of which covers only the adjacent finite element triangles, with basis functions of the support enlarged to the adjacent subdomains.

Note that since we consider only triangular or rectangular subdomains, the latter transformation of vertex basis functions is linear and the FEM coordinates of the transformed vertex basis functions are columns of $\begin{pmatrix} \mathbf{R}^E \\ \mathbf{I}^V \end{pmatrix}$, where $\mathbf{I}^V \in \mathbb{R}^{|I^V| \times |I^V|}$
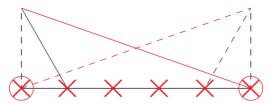
Figure 2. Extension of vertex basis functions (blue lines) to coarse-space basis functions (red lines) along an edge. In the adjacent subdomains the extension is discrete-harmonic, i.e., bilinear.

is the identity matrix and $\mathbf{R}^E \in \mathbb{R}^{|I^E| \times |I^V|}$ realizes the linear interpolation of the new vertex functions onto the interior nodes along the adjacent edges. Denoting by $\mathbf{I}^E \in \mathbb{R}^{|I^E| \times |I^E|}$ the identity matrix, the Schur complement is represented as follows:

$$\mathbf{S} = \begin{pmatrix} \mathbf{I}^E & \mathbf{0} \\ -\mathbf{R}^E & \mathbf{I}^V \end{pmatrix} \begin{pmatrix} \mathbf{S}_{I^E, I^E} & \widetilde{\mathbf{S}}_{I^E, I^V} \\ \widetilde{\mathbf{S}}_{I^V, I^E} & \widetilde{\mathbf{S}}_{I^V, I^V} \end{pmatrix} \begin{pmatrix} \mathbf{I}^E & -(\mathbf{R}^E)^T \\ \mathbf{0} & \mathbf{I}^V \end{pmatrix}.$$

In this representation, the matrix $\widetilde{\mathbf{S}}_{I^V, I^V}$ is nothing but the FEM discretization of the same bilinear form using the new vertex functions. This is why we shall denote it by $\mathbf{A}^H := \widetilde{\mathbf{S}}_{I^V, I^V}$. It gives rise to a spatial coarse-grid solver.

Finally, in the Schur complement approximation $\widehat{\mathbf{S}}$ we neglect the off-diagonal matrices $\widetilde{\mathbf{S}}_{I^V, I^E}, \widetilde{\mathbf{S}}_{I^E, I^V}$, and we also replace the edge-edge interaction matrix $\mathbf{S}_{I^E, I^E}$ by its block-diagonal part $\widehat{\mathbf{S}}_{I^E, I^E} := \operatorname{diag}(\mathbf{S}_{I_1^E, I_1^E}, \ldots, \mathbf{S}_{I_{N_E}^E, I_{N_E}^E})$. We arrive at the following representation of the approximate Schur complement inverse:

$$\widehat{\mathbf{S}}^{-1} = \sum_{i=1}^{N_E} (\mathbf{R}_{I_i^E, *}^E)^T (\mathbf{S}_{I_i^E, I_i^E})^{-1} \mathbf{R}_{I_i^E, *}^E + \begin{pmatrix} (\mathbf{R}^E)^T \\ \mathbf{I}^V \end{pmatrix} (\mathbf{A}^H)^{-1} \begin{pmatrix} \mathbf{R}^E & \mathbf{I}^V \end{pmatrix}.$$

The action of this matrix to a vector comprises the solution to N_E independent Dirichlet problems formulated on pairs of subdomains that are adjacent to a common skeleton edge. Further, the action of $\widehat{\mathbf{S}}^{-1}$ involves the solution of a coarse-grid problem arising from the same operator, which is now discretized by the FEM on the DDM skeleton grid. It is proven in [14] that the condition number of this preconditioned system is

$$\kappa(\widehat{\mathbf{S}}^{-1} \mathbf{S}) \leqslant C \Big(1 + \log \frac{H}{h} \Big)^2,$$

where C depends only on the shape of Ω, provided quasi-uniformity and shape-regularity of both the DDM decomposition and the FEM discretization and assuming that eventual jumps of bilinear form coefficients align with the DDM discretization.

3.2.2. 1-dimensional overlapping Schwarz DDM. We decompose the spatial interval $\Omega := (0, L)$ into N equidistant subintervals to which we add an overlap

$\delta \in (0, H)$, $H := L/N$, i.e., $\Omega_k := (\min\{(k-1)H - \delta, 0\}, \max\{kH + \delta, L\})$. The overlapping Schwarz DDM applied to a boundary value problem for an elliptic PDE, e.g., the following Dirichlet problem:

$$\begin{cases} -\operatorname{div}(\nu(x)\nabla u(x)) + m(x)u(x) = f(x), & x \in \Omega, \\ u(0) = u(L) = 0, \end{cases}$$

is an iterative procedure, where in the iterations $i = 1, 2, \ldots$ the following $k = 1, 2, \ldots, N$ Dirichlet auxiliary subproblems are solved in parallel:

$$(3.5) \quad \begin{cases} -\operatorname{div}(\nu(x)\nabla u_k^i(x)) + m(x)u_k^i(x) = f(x), & x \in \Omega_k, \\ u_k^i(kH - \delta) = u_{k-1}^{i-1}(kH - \delta), & k > 1, \\ u_k^i(kH + \delta) = u_{k+1}^{i-1}(kH + \delta), & k < N, \\ u_1^i(0) = u_N^i(L) = 0. \end{cases}$$

The problems (3.5) are discretized by the FEM with a step-size $h \ll H$.

4. Numerical experiments

We present three kinds of numerical results. In Section 4.1, we confirm the theoretically predicted convergence rates of the finite element semi-discretization combined with the two time-stepping schemes. In Section 4.2, we show robustness of the convergence of the parareal method with respect to the number of temporal subdomains. Finally, in Section 4.3 we display robustness of the combinations of the parareal with the Schur complement DDM in 2 dimensions as well as with the overlapping Schwarz method in 1 spatial dimension. In all these studies we shall consider problem (2.1) with the following setup:

$$(4.1) \qquad c(x) := 25, \ \nu(x) := 1, \ f(x, t) := 0, \ \Omega := (0, 1)^d, \ \Gamma_D := \Gamma,$$

$$\Gamma_N := \emptyset, \ T := 2, \ u_0(x) := \prod_{i=1}^{d} \sin(\pi x_i),$$

where $d \in \{1, 2\}$ is the spatial dimension.

4.1. Convergence of discretized solutions. We present convergence rates of the approximate solutions (2.6) using the backward Euler (2.5) and the Crank-Nicolson (2.7) time-stepping schemes in 1 spatial dimension at the final time $t := T$. The 1-dimensional, $d := 1$, exact solution to (2.1) with setup (4.1) is as follows:

$$(4.2) \qquad u(x, t) := \sin(\pi x)\mathrm{e}^{-\pi^2 t/c}.$$

184

We study the error of $u^{h,\delta t}(x, T) := u^h_m(x)$, which is the discretized solution (2.6) at time $T = m\delta t$. The spatial and temporal steps are equal, $h = \delta t$. As predicted by Theorem 2.4, in Table 1 we observe the quadratic convergence of the Crank-Nicolson scheme in the L^2-norm. The linear convergence of the backward Euler method guaranteed by Theorem 2.3 is becoming visible for fine discretizations, while for $h = \delta t < 1/64$ the error is in the pre-asymptotic phase.

$h = \delta t$	1/4	1/8	1/16	1/32	1/64	1/128	1/256
Euler	1.81e−2	2.22e−3	1.34e−3	1.10e−3	6.65e−4	3.62e−4	1.88e−4
eoc	—	3.03	0.73	0.28	0.73	0.88	0.94
Crank	2.96e−2	7.60e−3	1.91e−3	4.79e−4	1.20e−4	2.99e−5	7.48e−6
eoc	—	1.96	1.99	2.00	2.00	2.00	2.00

Table 1. Convergence in the L^2-norm $\|u(x, T) - u^{h,\delta t}(x, T)\|_{L^2(\Omega)}$ for the backward Euler and the Crank-Nicolson schemes for (4.2).

According to the theory, in Table 2 we show that the convergence in the H^1-seminorm is only linear in both cases. The quadratic convergence for the Crank-Nicolson scheme would require a higher-order finite element approximation in space. The experimental orders of convergence are computed as follows: $\mathrm{eoc}^h := \log_2(\mathrm{error}^{2h}/\mathrm{error}^h)$.

$h = \delta t$	1/4	1/8	1/16	1/32	1/64	1/128	1/256
Euler	2.26e−1	1.14e−1	5.76e−2	2.89e−2	1.45e−2	7.24e−3	3.62e−3
eoc	—	0.98	0.99	0.99	1.00	1.00	1.00
Crank	2.30e−1	1.15e−1	5.72e−2	2.86e−2	1.43e−2	7.15e−3	3.57e−3
eoc	—	1.01	1.00	1.00	1.00	1.00	1.00

Table 2. Convergence in the seminorm $|u(x, T) - u^{h,\delta t}(x, T)|_{H^1(\Omega)}$ for the backward Euler and the Crank-Nicolson schemes for (4.2).

We demonstrate the convergence for yet another example, which is now growing linearly in time:

$$(4.3) \qquad\qquad u(x, t) := \sin(\pi x)t.$$

The rest of the setup remains the same. In Table 3 we again observe the quadratic convergence of the Crank-Nicolson scheme in the L^2-norm, but now the corresponding convergence of the backward Euler scheme is also quadratic. This is because the time integrators preserve the linear time growth, hence, only the quadratic spatial FEM error is observed. In Table 4 we show that the convergence in the H^1-seminorm is linear in both cases. Due to the precise time integration a hardly any difference between the two integrators is observed.

$h = \delta t$	1/4	1/8	1/16	1/32	1/64	1/128	1/256
Euler	7.10e−2	1.71e−2	4.23e−3	1.05e−3	2.63e−4	6.56e−5	1.64e−5
eoc	—	2.05	2.02	2.01	2.00	2.00	2.00
Crank	6.97e−2	1.69e−2	4.21e−3	1.05e−3	2.62e−4	6.56e−5	1.64e−5
eoc	—	2.04	2.01	2.00	2.00	2.00	2.00

Table 3. Convergence in the L^2-norm $\|u(x,T) - u^{h,\delta t}(x,T)\|_{L^2(\Omega)}$ for the backward Euler and the Crank-Nicolson schemes for (4.3).

$h = \delta t$	1/4	1/8	1/16	1/32	1/64	1/128	1/256
Euler	9.97e−1	5.02e−1	2.52e−1	1.26e−1	6.30e−2	3.15e−2	1.57e−2
eoc	—	0.99	1.00	1.00	1.00	1.00	1.00
Crank	9.98e−1	5.02e−1	2.52e−1	1.26e−1	6.30e−2	3.15e−2	1.57e−2
eoc	—	0.99	1.00	1.00	1.00	1.00	1.00

Table 4. Convergence in the seminorm $|u(x,T) - u^{h,\delta t}(x,T)|_{H^1(\Omega)}$ for the backward Euler and the Crank-Nicolson schemes for (4.3).

4.2. Robustness of parareal. We fix the spatial and temporal discretization steps, $h := 1/32$ and $\delta t := 1/512$, respectively, and we choose the backward Euler scheme. We shall study the following L^2-error of the parareal iterations,

$$(4.4) \qquad \frac{\|u_{\text{parareal}}^{h,\delta t,\Delta T,i}(x,T) - u^{h,\delta t}(x,T)\|_{L^2(\Omega)}}{\|u^{h,\delta t}(x,T)\|_{L^2(\Omega)}},$$

where

$$u_{\text{parareal}}^{h,\delta t,\Delta T,i}(x,T) := \sum_{j=1}^{n} (\mathbf{U}_M^i)_j \varphi_j(x),$$

which is the approximation (3.3) of the ith iteration of the parareal method at the time $T = M\Delta T$. In Table 5 we can see that in order to achieve a given precision (e.g., 1e−8) the number of iterations decreases ($i = 6, 5, 5$) with an increasing parallelism in time ($\Delta T = 1/4, 1/8, 1/16$). This means that the overall complexity of the predictor steps enjoys optimal parallel scalability. In practice, the parallel speedup is partly deteoriated by the sequential corrector steps.

ΔT	$i := 1$	$i := 2$	$i := 3$	$i := 4$	$i := 5$	$i := 6$
1/2	2.04e−1	1.28e−2	2.62e−4	0	0	0
1/4	1.28e−1	6.72e−3	1.93e−4	3.33e−6	3.86e−8	1.87e−9
1/8	7.08e−2	2.28e−3	4.52e−5	6.20e−7	8.10e−9	1.29e−9
1/16	3.70e−2	6.53e−4	7.41e−6	6.09e−8	5.18e−10	5.78e−11

Table 5. Relative error (4.4) of parareal iterations for the $2d$ problem.

4.3. Robustness of DDM coupled with parareal. Finally, we present numerical results of the novel combination of the parareal method coupled with the Schur complement DDM in 2 spatial dimensions. Again, we fix the spatial and temporal discretization steps, $h := 1/32$ and $\delta t := 1/512$, respectively, and we choose the backward Euler scheme. We shall study error (4.4) of the parareal iterations, but now the arising linear systems (2.5) are solved by the preconditioned conjugate gradients (PCG) method up to the relative precision 1e−8 using the Schur complement DDM preconditioner of Section 3.2.1. The results in Table 6 show the error after three parareal iterations. We observe that the convergence in the column $i := 3$ of Table 5 is not affected. Moreover, the convergence is independent of the spatial parallelism and it is again improving with the increasing parallelism in time. Note that the maximal numbers of PCG iterations were 6, 15, 27, and 21, respectively, for the DDM parameters $H := 1/2, 1/4, 1/8,$ and $1/16$.

ΔT	$H := 1/2$	$H := 1/4$	$H := 1/8$	$H := 1/16$
1/2	2.62e−4	2.62e−4	2.62e−4	2.62e−4
1/4	1.92e−4	1.92e−4	1.92e−4	1.92e−4
1/8	4.40e−5	4.40e−5	4.40e−5	4.40e−5
1/16	6.95e−6	6.95e−6	6.96e−6	6.95e−6

Table 6. Relative error (4.4) after 3 parareal-DDM iterations in $2d$ when fixing the relative precision of the underlying PCG to 1e−8.

In Table 7 we show that the convergence of the parareal method is slightly deteriorated when relaxing the relative precision of the nested PCG method to 1e−6. This leads to more iterations of the parareal method, which is compensated by lower numbers of PCG iterations, namely, 5, 14, 18, and 13, respectively, for the DDM parameters $H := 1/2, 1/4, 1/8,$ and $1/16$.

ΔT	$H := 1/2$	$H := 1/4$	$H := 1/8$	$H := 1/16$
1/2	2.62e−4	2.62e−4	2.64e−4	2.63e−4
1/4	1.92e−4	1.92e−4	1.94e−4	1.93e−4
1/8	4.41e−5	4.42e−5	5.57e−5	5.01e−5
1/16	7.75e−6	8.32e−6	3.58e−5	2.50e−5

Table 7. Relative error (4.4) after 3 parareal-DDM iterations in $2d$ when fixing the relative precision of the underlying PCG to 1e−6.

In Tables 8 and 9 we present results of 1-dimensional counterparts to Tables 6 and 7. Here we fix the discretization steps to $h := 1/256$ and $\delta t := 1/512$ and we choose the backward Euler scheme. We combine the parareal method with the

1-dimensional overlapping Schwarz DDM of Section 3.2.2 for the approximate solution to the auxiliary linear systems (2.5). In the Schwarz method, we fix the overlap to $\delta := H/4$. The results listed in Table 8 show the error after three parareal iterations. Similarly to the $2d$ case we observe that the convergence of parareal is improving with increasing time parallelism. We can also see that the convergence is influenced by the precision (relative residual error) of the Schwarz method, which we alternate between 1e−8 in Table 8 and 1e−6 in Table 9. The faster convergence of the parareal method is compensated by the higher number of underlying Schwarz iterations. Namely, when fixing the relative precision of Schwarz iterations to 1e−8, we observe 1, 2, 3, 6, and 12 Schwarz iterations for $H := 1/2$, $1/4$, $1/8$, $1/16$, and $1/32$, respectively. For the relative precision 1e−6, the respective numbers of Schwarz iterations decreases to 1, 1, 2, 4, and 9.

ΔT	$H := 1/2$	$H := 1/4$	$H := 1/8$	$H := 1/16$	$H := 1/32$
1/16	2.56e−10	2.56e−10	2.48e−10	2.19e−10	3.75e−10
1/32	1.60e−11	1.62e−11	6.78e−12	2.22e−11	6.17e−10
1/64	8.99e−13	1.03e−12	1.00e−11	3.89e−11	6.35e−10
1/128	1.25e−13	2.55e−13	1.37e−11	4.27e−11	6.40e−10
1/256	9.86e−14	2.31e−13	1.77e−11	4.82e−11	6.51e−10

Table 8. Relative error (4.4) after 3 parareal-DDM iterations in $1d$ when fixing the precision of the underlying Schwarz method to 1e−8.

ΔT	$H := 1/2$	$H := 1/4$	$H := 1/8$	$H := 1/16$	$H := 1/32$
1/16	2.56e−10	3.40e−9	1.09e−8	4.44e−8	8.44e−8
1/32	1.60e−11	4.69e−9	1.22e−8	4.55e−8	8.48e−8
1/64	8.99e−13	6.34e−9	1.43e−8	4.73e−8	8.51e−8
1/128	1.25e−13	8.49e−9	1.80e−8	5.09e−8	8.58e−8
1/256	9.86e−14	1.10e−8	2.31e−8	5.73e−8	8.72e−8

Table 9. Relative error (4.4) after 3 parareal-DDM iterations in $1d$ when fixing the precision of the underlying Schwarz method to 1e−6.

5. Conclusion

In this paper we dealt with a combination of the parareal and domain decomposition methods for the transient heat equation in 1 and 2 spatial dimensions. We recalled the convergence theory of the FEM semi-discretization and two time-stepping schemes and we confirmed the theory by numerical experiments in $1d$. Further, we recalled the parareal method, the $2d$ vertex-based Schur complement DDM, and the $1d$ overlapping Schwarz DDM. We presented novel combinations of the parareal and DDM with numerical results indicating robustness of the new method.

The message of our paper is that the convergence of parareal is not affected by the underlying inexact DDM solver, provided its accuracy is related to that of the parareal method. To the best of our knowledge, this robustness of the parareal method with respect to inexact local solves has not been studied in the literature yet. Both our combinations of the parareal and $2d$ vertex-based Schur complement DDM or $1d$ overlapping Schwarz DDM on multiple subdomains are novel. The combination with Schwarz DDM has been previously presented in [15], [16] only for two spatial subdomains.

This paper is intended as an initial study. However, massively parallel simulations are needed, which will be, together with space-time Galerkin approach, presented in the near future.

References

[1] *J. H. Bramble, J. E. Pasciak, A. H. Schatz*: The construction of preconditioners for elliptic problems by substructuring. I. Math. Comput. *47* (1986), 103–134. `zbl` `MR` `doi`

[2] *X. Dai, Y. Maday*: Stable parareal in time method for first- and second-order hyperbolic systems. SIAM J. Sci. Comput. *35* (2013), A52–A78. `zbl` `MR` `doi`

[3] *R. D. Falgout, S. Friedhoff, T. V. Kolev, S. P. MacLachlan, J. B. Schroder*: Parallel time integration with multigrid. SIAM J. Sci. Comput. *36* (2014), C635–C661. `zbl` `MR` `doi`

[4] *C. Farhat, M. Chandesris*: Time-decomposed parallel time-integrators: theory and feasibility studies for fluid, structure, and fluid-structure applications. Int. J. Numer. Methods Eng. *58* (2003), 1397–1434. `zbl` `MR` `doi`

[5] *C. Farhat, F.-X. Roux*: A method of finite element tearing and interconnecting and its parallel solution algorithm. Int. J. Numer. Methods Eng. *32* (1991), 1205–1227. `zbl` `MR` `doi`

[6] *M. J. Gander*: 50 years of time parallel time integration. Multiple Shooting and Time Domain Decomposition Methods (T. Carraro et al., eds.). Contributions Mathematical and Computational Sciences 9, Springer, Cham, 2015, pp. 69–113. `zbl` `MR` `doi`

[7] *M. J. Gander, L. Halpern, F. Nataf*: Optimal Schwarz waveform relaxation for the one dimensional wave equation. SIAM J. Numer. Anal. *41* (2003), 1643–1681. `zbl` `MR` `doi`

[8] *M. J. Gander, Y.-L. Jiang, R.-J. Li*: Parareal Schwarz waveform relaxation methods. Domain Decomposition Methods in Science and Engineering XX (R. Bank et al., eds.). Lectures Notes in Computational Science and Engineering 91, Springer, Berlin, 2013, pp. 451–458. `zbl` `MR` `doi`

[9] *M. J. Gander, F. Kwok, B. C. Mandal*: Dirichlet-Neumann and Neumann-Neumann waveform relaxation algorithms for parabolic problems. ETNA, Electron. Trans. Numer. Anal. *45* (2016), 424–456. `zbl` `MR`

[10] *M. J. Gander, M. Neumüller*: Analysis of a new space-time parallel multigrid algorithm for parabolic problems. SIAM J. Sci. Comput. *38* (2016), A2173–A2208. `zbl` `MR` `doi`

[11] *M. J. Gander, S. Vandewalle*: Analysis of the parareal time-parallel time-integration method. SIAM J. Sci. Comput. *29* (2007), 556–578. `zbl` `MR` `doi`

[12] *M. J. Gander, S. Vandewalle*: On the superlinear and linear convergence of the parareal algorithm. Domain Decomposition Methods in Science and Engineering XVI (O. B. Widlund et al., eds.). Lectures Notes in Computational Science and Engineering 55, Springer, Berlin, 2007, pp. 291–298. `zbl` `MR` `doi`

[13] *J.-L. Lions, Y. Maday, G. Turinici*: Résolution d'EDP par un schéma en temps "pararéel". C. R. Acad. Sci., Paris, Sér. I, Math. *332* (2001), 661–668. (In French.) `zbl` `MR` `doi`

[14] *D. Lukáš, J. Bouchala, P. Vodstrčil, L. Malý*: 2-dimensional primal domain decomposition theory in detail. Appl. Math., Praha *60* (2015), 265–283. `zbl` `MR` `doi`

[15] *Y. Maday*: The 'parareal in time' algorithm. Substructuring Techniques and Domain Decomposition Methods (F. Magoulès, ed.). Computational Science, Engineering and Technology Series 24, Saxe-Coburg Publications, Stirling, 2010, pp. 19–44. `doi`

[16] *Y. Maday, G. Turinici*: The parareal in time iterative solver: a further direction to parallel implementation. Domain Decomposition Methods in Science and Engineering (T. J. Barth et al., eds.). Lectures Notes in Computational Science and Engineering 40, Springer, Berlin, 2005, pp. 441–448. `zbl` `MR` `doi`

[17] *J. Mandel, M. Brezina*: Balancing domain decomposition for problems with large jumps in coefficients. Math. Comput. *65* (1996), 1387–1401. `zbl` `MR` `doi`

[18] *D. Mercerat, L. Guillot, J.-P. Vilotte*: Application of the parareal algorithm for acoustic wave propagation. AIP Conf. Proc. *1168* (2009), 1521–1524. `doi`

[19] *M. Neumüller*: Space-Time Methods: Fast Solvers and Applications. Monographic Series, Graz University of Technology, Graz, 2013.

[20] *S. Schöps, I. Niyonzima, M. Clemens*: Parallel-in-time simulation of eddy current problems using parareal. IEEE Trans. Magn. *54* (2018), Article No. 7200604, 1–4. `doi`

[21] *B. F. Smith, P. E. Bjørstad, W. D. Gropp*: Domain Decomposition. Parallel Multilevel Methods for Elliptic Partial Differential Equations. Cambridge University Press, Cambridge, 1996. `zbl` `MR`

[22] *V. Thomée*: Galerkin Finite Element Methods for Parabolic Problems. Springer Series in Computational Mathematics 25, Springer, Berlin, 2006. `zbl` `MR` `doi`

[23] *A. Toselli, O. Widlund*: Domain Decomposition Methods—Algorithms and Theory. Springer Series in Computational Mathematics 34, Springer, Berlin, 2005. `zbl` `MR` `doi`

[24] *E. Zeidler*: Nonlinear Functional Analysis and Its Applications. II/A: Linear Monotone Operators. Springer, New York, 1990. `zbl` `MR` `doi`

Authors' address: *Ladislav Foltyn*, *Dalibor Lukáš* (corresponding author), *Ivo Peterek*, Department of Applied Mathematics, Faculty of Electrical Engineering and Computer Science & IT4Innovations, VŠB-Technical University of Ostrava, 17. listopadu 15, 708 00 Ostrava-Poruba, Czech Republic, e-mail: `ladislav.foltyn@vsb.cz`, `dalibor.lukas @vsb.cz`, `ivo.peterek@vsb.cz`.